Supplemental Data

The Brain in Chronic CRPS Pain: Abnormal Gray-White Matter Interactions in Emotional and Autonomic Regions

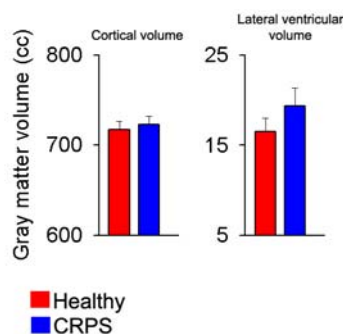Paul Y. Geha, Marwan N. Baliki, R. Norman Harden, William R. Bauer, Todd B. Parrish, and A. Vania Apkarian

Figure S1. Whole-brain neocortical gray matter, white matter, and lateral ventricle sizes did not differ between CRPS and control subjects. Histograms show mean and SEMs. Skull-normalized whole-brain neocortical gray matter volume (excluding the cerebellum, deep gray matter, and brainstem; SIENAX analysis) was 723 ± 10 cm^3 (mean $\pm$ SEM; n = 22) in the CRPS brain and 717 ± 10 cm^3 (n = 22) in the healthy brain (unpaired t-test, p>0.65), matched for age and sex. White matter volume was 672 ± 8 cm^3 (n=22) in the CRPS brain, and 671 ± 8 cm^3 (n=22) in the healthy brain (p>0.9). Lateral ventricular volume in the CRPS brain was 19 ± 2 cm^3 (mean $\pm$ SEM; n = 22) and 17 ± 2 cm^3 in the healthy brain (n = 22) (p>0.25).
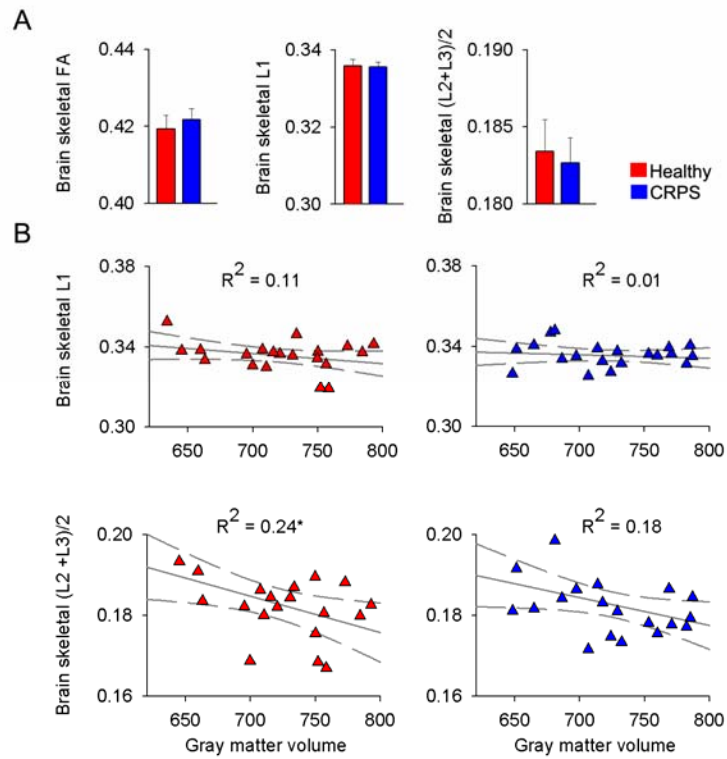
Figure S2. Whole-brain skeletal anisotropy (FA), parallel (λ1) and perpendicular (λ2+λ3)/2 diffusivity, and their relationship to whole-brain gray matter are shown. **(A)** Histograms are means and SEMs. There were no differences between the groups in mean whole-brain skeletal FA (CRPS patients FA = 0.419 ± 0.004, and in healthy controls FA = 0.421 ± 0.003), mean brain parallel (CRPS, λ1 = 0.336 ± 0.002; Healthy, λ1 = 0.336 ± 0.001) and perpendicular diffusivities (CRPS, (λ2+λ3)/2 = 0.183 ± 0.003; Healthy, (λ2+λ3)/2 = 0.183 ± 0.003). **(B)** Only the perpendicular diffusivity in healthy subjects showed a significant correlation with whole-brain gray matter volume.
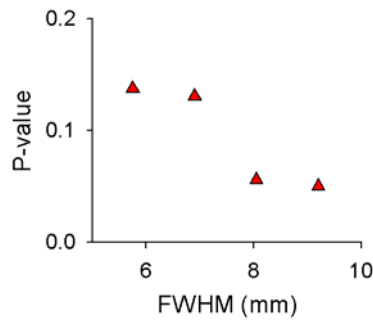*p < 0.05.*

Figure S3. The p-value of the gray matter cluster showing a significant difference between healthy and CRPS subjects in the VBM analysis improved with smoothing. Hence we chose the smoothing kernel with full-width half maximum (FWHM) = 9.2 mm.
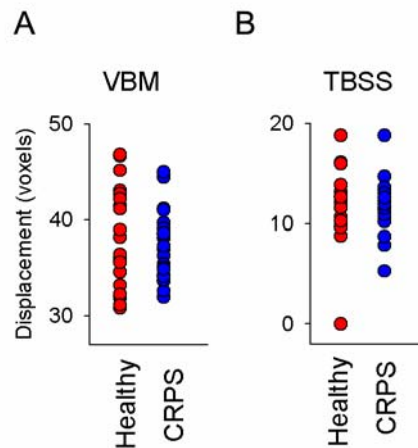

Figure S4. Head displacement corrections did not differ between CRPS and control subjects in either VBM or TBSS (DTI-based) analyses. Non-linear displacement scores in voxel units for the registration of each subject's T1 images to the target image in VBM analysis (**A**) and FA images to the target image in the tracts based spatial statistics (TBSS) (**B**) are not different between healthy (red) and CRPS subjects (blue). **(A)** We generated a study specific template for the VBM analysis; hence all the displacements are greater than zero. **(B)** The target DTI image is one of the healthy subjects shown at displacement = zero. These data indicate that registration differences cannot account for gray matter (VBM) or white matter (TBSS) analyses results.
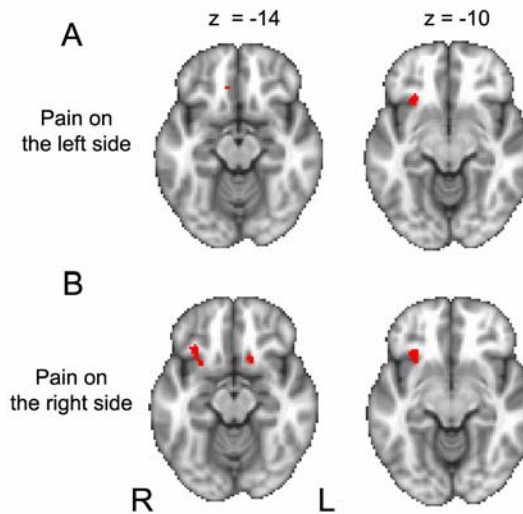
Figure S5. The right anterior insula shows decreased gray matter density after subdividing the CRPS patient population to ones with only left-sided body pain **(A)** or only right-sided body pain **(B).** These analyses were restricted to a gray matter mask including the cluster showing a group effect on the right side when using all patients (from Figure 2A) and its mirror image on the left side. **(A)** VBM comparison between CRPS and matched healthy controls including only 9 patients with left-sided body pain in comparison to their matched healthy controls. Decreased gray matter density is observed in the right VMPFC and AI (n = 9 per group, $p < 0.05$ corrected) **(B)** VBM comparison between 7 patients with right sided body pain and their matched healthy controls showed two clusters with a significant decrease in gray matter density in CRPS in the right AI/inferior frontal gyrus and part of the left VMPFC (n = 7 per group, $p < 0.05$ corrected). Therefore, gray matter atrophy seems right hemisphere dominant, independent of body side location for CRPS pain.
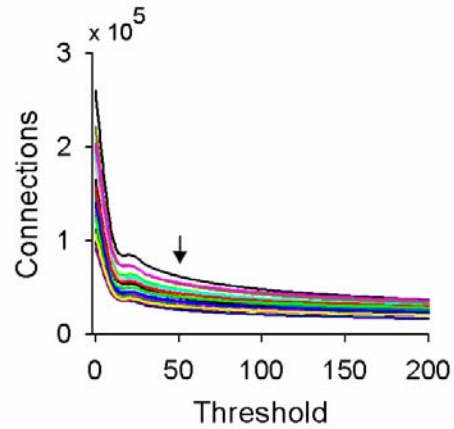
Figure S6. Data used to establish a threshold in probabilistic tractography for declaring a voxel connected to the seed. From each seed voxel, 5000 samples were drawn to build the *a posteriori* distribution of the connectivity distribution. Hence, the number of samples passing through each voxel is proportional to the probability of connection between the seed and that voxel. The Figure shows the total count of voxels throughout the brain connected to the seed as a function of the number of samples observed per voxel (threshold), plotted for each of the healthy subject (n = 21). Given that the dependence stabilizes at higher number of samples observed per voxel, we chose 50 samples as the threshold to declare the presence of a connection, and used this threshold to quantify connections.
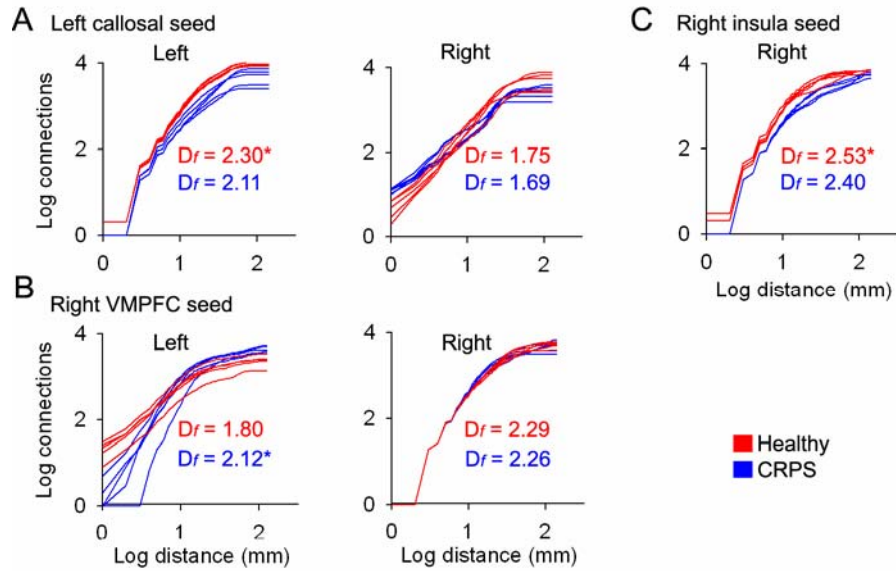
Figure S7. Log-log relationship of cumulative connections as a function of distance for the callosal seed with decreased FA in CRPS patients (**A**), the right VMPFC (**B**), and right AI seed (**C**). Data from only 5 patients and 5 healthy controls are plotted for the sake of illustration. There is a distance scaling range within which connectivity follows a well-defined log-log slope, which identifies the fractal branching properties of these connections. Both the scaling range and the fractal D_f dimensions showed significant differences between CRPS patients and healthy matched controls.
* p <0.05, unpaired t-test comparing patients and healthy controls.
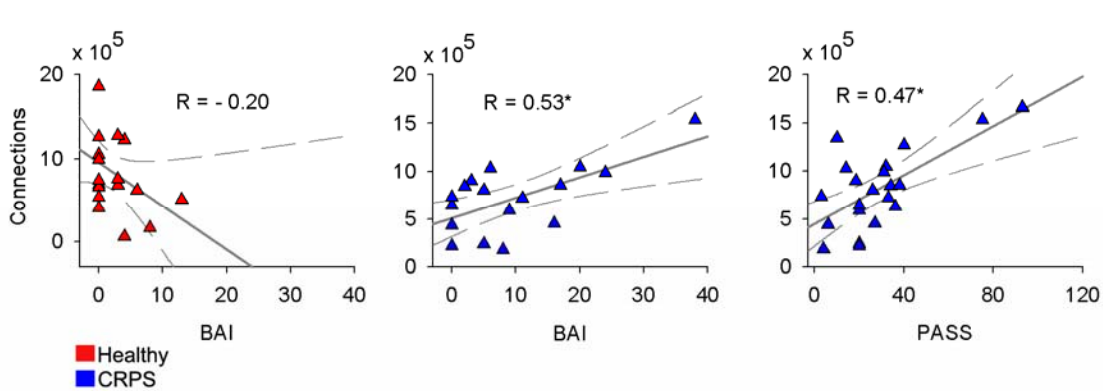
	Seed	R VMPFC		R AI		R NAc	
Target		Healthy	CRPS	Healthy	CRPS	Healthy	CRPS
R VMPFC				1 ± 94	5 ± 48	$(5.6 \pm 3.9) \times 10^5$	$(5.8 \pm 3.8) \times 10^5$
R AI		2 ± 11	16 ± 140			20 ± 333	5 ± 52
R NAc		$(6.9 \pm 6.0) \times 10^5$	$(8.0 \pm 4.4) \times 10^5$	$(0.1 \pm 2.9) \times 10^4$	21 ± 335		
Numbers are median ± quartiles; Abbreviations: VMPFC = ventromedial prefrontal cortex; AI = anterior insula; NAc = nucleus accumbens; numbers highlighted in red are significantly different, using Mann-Whitney U test, p < 0.01.							

Figure S8. Strength of white matter connections between right VMPFC and right NAc are related to anxiety in CRPS. Spearman Rank correlation between anxiety scores from the Beck's Anxiety Index (BAI) (left 2 panels) and the probabilistic white matter connections between the R VMPFC and the R NAc is significant only in patients. Last panel depicts the Spearman Rank correlation between the same connections and the Pain Anxiety Symptom Scale (PASS) in CRPS patients. The table shows the seed to seed probabilistic connections for the three different areas showing a decrease in gray matter density in CRPS. The VMPFC to NAc connection values are highlighted in italic. Numbers in red show significant change between CRPS and healthy controls (p < 0.01). Note that these seed to seed connectivity counts replicate results we see for seed to whole anatomical target connectivity. Seed to seed R VMPFC to R AI connectivity is increased in CRPS similar to the increase observed between R VMPFC and whole R AI target (**Figure 4C**); and seed to seed decreased connectivity from R AI to R NAc replicates results for whole basal ganglion target from R AI seed (**Figure 5C**).
* p < 0.05

	Pain (VAS)	Duration (years)	Location	Inciting event	Symptoms and signs	BDI	BAI	PASS	MQS
					Supplementary Table 1a. CRPS patients' clinical characteristics				
PF21	4.3	5.25	Bilateral knees	Post-knee surgery	Sweating, changing skin color, allodynia	10	--	36	26
PF25	6.4	1.8	Right knee, leg and foot	None	Swelling, change in skin color and temperature	16	12	43	47.6
PF26b	6.6	1.6	Left ankle	post-surgery	Swelling, itching, change in skin color and temperature, LRM, allodynia	13	38	75	0
PF26c	2	0.4	Right arm	post-accident	Swelling, change in skin color and temperature, LRM, allodynia	13	3	18.5	14.7
PF26d	4.8	1	Left toe/foot and ankle	Post-accident	Swelling, change in skin color and temperature, LRM, allodynia	7	20	32	19.3
PF28b	2.3	1.7	Left foot/spreading to whole body	Post-surgery	Swelling, change in skin color and temperature, LRM, allodynia	5.5	8	4	0
PF28	9.8	2.5	Bilateral legs and back	Post-accident	Sweating, changing skin color, muscle atrophy, allodynia	27	--	93	34.5
PF31	3.7	0.4	Left arm	Post-accident	Swelling, change in skin color temperatures, LRM, allodynia	5	0	6	9.3
PF32	1.5	6.1	Left arm and hip	None	Allodynia, swelling, change in skin color and temperature	5	1	19	62.2
PF35	2.4	2.4	Bilateral feet	Post-accident	Changing skin color, abnormal nail growth, allodynia	17	--	40	8
PF39	6.6	1.3	Right hand, wrist, ankle and foot	Post-accident	Swelling, change in skin color and temperature, allodynia	9	2	34	54.9
PF40	8.2	13.5	Left arm and hand	Post-accident	Swelling, change in skin color temperatures, LRM, allodynia	10	16	27	27.5
PF41b	8.8	3.5	Left foot	Post-accident	Swelling, changing skin color, allodynia	12	9	20	36.3
PF43	5.6	5	Bilateral hands, arms, legs and feet	None	Swelling, changing skin color and temperature, allodynia	14	17	38	35.6
PF44	7.2	1.1	Left hand and arm	Post-surgery	Changing skin temperature, swelling	1	0	7	6.6
PF46	5.4	0.4	Bilateral hands	Post-accident	Changing skin color, swelling, allodynia	11	5	20	24.5
PF47	9.7	7.9	Left leg and foot	Post-accident	Swelling, changing skin temperature, allodynia	14	0	20	29
PF47b	6.4	8	Right neck	Post-accident	Allodynia, changing skin temperature	2	4	7	15.6
PF47c	7.3	7.3	Bilateral arms, chest and back	None	Swelling, changing skin temperature, allodynia	13	5	26	25.6
PF50b	7.5	3.1	Left ankle, right hand	Post-accident	Changing skin color and temperature, swelling, LRM allodynia	12	--	10	44
PF53	7.7	0.3	Right foot	Post-accident	Changing skin temperature, swelling, allodynia	5	0	3	0
PF59	6.8	1.5	Right arm and hand	Post-accident	Allodynia, changing skin color temperature	6	1	2	11.2
PF61	8.2	0.25	Bilateral arms and hands	None	Swelling, change in skin temperatures, allodynia	6	6	14	16.8
PM36	6.1	0.5	Right elbow	Post-accident	Swelling, change in skin color and temperature, LRM, allodynia	6	24	31	0
PM48	2.9	1.4	Left foot	Post-accident	Swelling, abnormal nail growth, allodynia	13	0	20	8.5
PM56	2.2	0.25	Bilateral Neck and arms	None	Swelling, change in temperature, limited range of motion, allodynia	12	11	33	0

In the healthy control subjects mean BDI $\pm$ sem = 1.2 $\pm$ 0.4 and mean BAI $\pm$ sem = 1.8 $\pm$ 0.5.
Empty cells indicate missing data.
Abbreviations: VAS, visual analogue scale; BDI, Beck's Depression Index; BAI, Beck's anxiety index; PASS, Pain Anxiety Symptom Scale; MQS, medication quantification scale.

Supplementary Table 1b. CRPS patients' clinical characteristics

	SEX	Hand-edness	Medication	MQS	VBM	DTI
PF21	F	R	ibuprofen, ultram, vicodin, zoloft	26	No	Yes
PF25	F	R	neurontin, elavil, topamax, lidoderm, xanax, relpax, percocet, vicodin, morphine	47.6	Yes	No
PF26b	F	R		0	Yes	Yes
PF26c	F	R	lyrica, mysoline	14.7	Yes	Yes
PF26d	F	R	zonegran, celebrex, relpax, protanix, timolol	19.3	Yes	Yes
PF28b	F	R		0	Yes	Yes
PF28	F	R	baclofen, methadone, effexor xr, gabapentin, zanaflex, phenobarbital	34.5	No	Yes
PF31	F	R	trileptal, ultram, gabapentin	9.3	Yes	Yes
PF32	F	R	levothyroxin, lyrica, tramadol, darvocet, ibuprofen, xanaflex, cymbalta, rozerem, trileptal, methadone	62.2	Yes	No
PF35	F	R	neurontin, elavil	8	No	Yes
PF39	F	R	Lyrica, vicodin, neurontin,, methadone, ultram, ibuprofen, lidoderm, zanaflex	54.9	Yes	Yes
PF40	F	R	soma, lyrica, ambian cr, darvocet	27.5	Yes	Yes
PF41b	F	R	soma, zocor, vicodin, lidoderm, topamax, vallium, demerol, vistaril, synthroid, percocet	36.3	Yes	Yes
PF43	F	R	vicodin, lamictal, gabatril, trazodone, dibenzyline	35.6	Yes	Yes
PF44	F	R	trileptal, lyrica	6.6	Yes	No
PF46	F	L-R	wellbutrin, lyrica, lidoderm, clonazepam	24.5	Yes	Yes
PF47	F	R	percocet, zoloft, keppra, trileptal, flexeril, toradol, remeron	29	Yes	Yes
PF47b	F	R	premarin, motrin, indocin	15.6	Yes	No
PF47c	F	R	methadone, cymbalta, zanaflex, lyrica	25.6	Yes	Yes
PF50b	F	R	vicodin, darvocet, lyrica, flexeril	44	Yes	Yes
PF53	F	R		0	Yes	Yes
PF59	F	L	macrodantin, excedrin	11.2	Yes	No
PF61	F	R	trileptal, celebrex, cymbalta, zanaflex, lyrica	16.8	Yes	Yes
PM36	M	R		0	Yes	Yes
PM48	M	R	lyrica, trileptal	8.5	Yes	Yes
PM56	M	R		0	No	Yes

In the healthy control subjects mean BDI $\pm$ sem = 1.2 $\pm$ 0.4 and mean BAI $\pm$ sem = 1.8 $\pm$ 0.5.
Abbreviations: VAS, visual analogue scale; BDI, Beck's Depression Index; BAI, Beck's anxiety index; PASS, Pain Anxiety Symptom Scale; MQS, medication quantification scale.

Supplementary Table 2. White matter total number of connections, fractal dimension and associated scaling ranges calculated from three seeds, one derived from white matter region with decreased FA in CRPS, and the others derived from gray matter areas showing decreased density in CRPS.

Seeds		Left hemisphere		Right hemisphere	
		Healthy	CRPS	Healthy	CRPS
L callosal mask	Total connections	8873.0 ± 341.9	6694.8± 386.9	3646.2 ± 340.4	3570.1± 321.6
	Fractal dimension	2.30± 0.02	2.11± 0.02	1.75 ± 0.04	1.69 ± 0.03
	Scaling range (mm)	20.0 ± 1.1	28.5± 2.6	39.1± 2.4	40.7 ± 1.6
R AI	Total connections	178 ± 16.4	132.1 ± 34.8	6542.2 ± 170.2	6034.3 ± 135.1
	Fractal dimension	N/A	N/A	2.53 ± 0.03	2.40 ± 0.02
	Scaling range (mm)	N/A	N/A	14.3 ± 0.7	18.1± 0.9
R VMPFC	Total connections	2874.4 ± 176.7	3309.9 ± 307.8	5291.3 ± 200.9	4468.5 ± 263.3
	Fractal dimension	1.80 ± 0.07	2.12± 0.01	2.29 ± 0.03	2.26 ± 0.02
	Scaling range (mm)	20.2 ± 1.1	21.7 ± 5.3	19.8 ± 1.1	18.1 ± 0.9

Total connections are shown as median ± quartiles; fractal dimension and scaling range are mean ± SEMs. Numbers highlighted in red are significantly different using unpaired (non-parametric for connections, and parametric for fractal dimensions and scaling rages) t-test, $p < 0.05$.
Abbreviations: FA, fractional anisotropy; AI, anterior insula; VMPFC, ventromedial prefrontal cortex; R, right; L, left.

Supplementary Table 3. Relationships between clinical characteristics for CRPS

	Pain (VAS)	Duration (Years)	Age (Years)	BDI	BAI	PASS	MQS
Pain (VAS)	1.000	0.336	0.624	0.124	-0.158	-0.029	0.230
Duration (Years)	0.336	1.000	0.045	0.376	0.227	0.265	0.417
Age	0.624	0.045	1.000	-0.201	-0.423	-0.489	0.005
BDI	0.124	0.376	-0.201	1.000	0.434	0.666	0.439
BAI	-0.158	0.227	-0.423	0.434	1.000	0.690	0.011
PASS	-0.029	0.265	-0.489	0.666	0.690	1.000	0.406
MQS	0.230	0.417	0.005	0.439	0.011	0.406	1.000

Correlations were calculated non-parametrically by Spearman Rank; red represents $p<0.05$; For abbreviations see Supplementary Table 1